Journal of Big Data

RESEARCH Open Access

Deep learning enables the quantification of browning capacity of human adipose samples

Yuxin Wang[1†], Shiman Zuo[1†], Nanfei Yang[1], Ani Jian[1], Wei Zheng[1], Zichun Hua[2*] and Pingping Shen[1,3*]

[†]Yuxin Wang and Shiman Zuo have contributed equally to this study.

*Correspondence: huazc@nju.edu.cn; ppshen@nju.edu.cn

[1] Department of Urology, Nanjing Drum Tower Hospital, The Affiliated Hospital of Nanjing University Medical School and State Key Laboratory of Pharmaceutical Biotechnology, School of Life Sciences, Nanjing University, Nanjing 210023, China
[2] State Key Laboratory of Pharmaceutical Biotechnology, School of Life Sciences, Nanjing University, Nanjing 210023, China
[3] Shenzhen Research Institute of Nanjing University, Shenzhen 518000, China

Abstract

Background: The recruitment of thermogenic adipocytes in human fat depots markedly improves metabolic disorders such as type 2 diabetes mellitus (T2DM). However, identification and quantification of thermogenic cells in human fats, especially in metabolic disorders patients, remains a major challenge. Here, we aim to provide a stringent validation of human thermogenic adipocyte signature genes, and construct transcriptome-based models to quantify the browning degree of human fats.

Methods: Evidence from RNA-seq, microarray analyses and experimental approaches were integrated to isolate robust human brown-like fat signature genes. Meta-analysis was employed to validate the performance of known human brown-like fat marker genes. Autoencoder was used to reveal the browning levels of human adipose samples for supervised machine learning. Ensemble machine learning was applied to devised molecular metrics for quantifying browning degree of human fats. Obesity and T2DM datasets were used to validate the performance of the molecular metrics in adipose-related metabolic disorders.

Results: Human brown-like adipocytes were heterogeneous populations which showed distinct transcriptional patterns and biological features. Only *DHRS11*, *REEP6* and *STX11* were robust signature genes that were consistently up-regulated in different human brown-like fats, especially in creatine-induced UCP1-independent adipocytes. The molecular metrices based on the expression patterns of the three signature genes, named human browning capacity index (HBI) and absolute HBI (absHBI), were superior to 26 traditional human brown-like fat marker genes and previously reported browning classifier in prediction of browning levels of human adipocytes and adipose tissues as well as primary cell cultures upon various physiological and pharmacological stimuli. Notably, these molecular metrics also reflected the insulin sensitivity and glucose-lipid metabolic activity of human adipose samples from obesity and T2DM patients.

Conclusions: In summary, this study provides promising signatures and computational tools for evaluating browning levels of human adipose samples in response to physiological and medical intervention. The metrices construction pipeline provides an alternative approach for training machine learning models using unlabeled samples.

Keywords: Human brown-like fat, Molecular metrics, Ensemble machine learning, Type 2 diabetes mellitus

Background

Mammals possess two main types of fats, named white and brown adipose tissues [1]. White adipose tissue (WAT) is specialized for lipid storage and release, while brown adipose tissue (BAT) expends nutritional energy in the form of heat for non-shivering thermogenesis. Although WAT and BAT are functional different adipose tissues, brown-like, thermogenic fat cells can be detected in various WAT depots in response to cold exposure and certain other stimuli [1, 2]. These cells have consequently been termed beige or brite (brown-in-white) adipocytes. Importantly, adult humans also possess thermogenic adipocytes in the supraclavicular and neck region as well as in multiple WAT depots upon exposure to cold stimuli or β-adrenergic receptor agonist [3, 4].

Emerging evidence suggests that promoting the recruitment of brown-like cells in WAT depots improves metabolic health in ways far beyond the induction of thermogenesis in both rodents and humans [1, 5]. For instance, selective induction of white adipocytes browning improves insulin sensitivity and correct hyperlipidemia [6–8], whereas impaired beige fat biogenesis leads to systemic glucose tolerance and insulin resistance [9, 10]. Current physiological and medical interventions based on browning induction, such as cold stimulation and thiazolidinedione treatment, provide promising therapeutic measures to improve metabolic disorders. The efficacy evaluation of these measures is highly relied on the accurate estimation of the levels of adipose browning. Thus, a robust quantification method for beige fat biogenesis on human WATs would predict clinical outcome and lead to the development of therapeutic measures that improve metabolic health [4].

However, it remains challenging in the quantification of human brown and beige cells. The most likely explanation is that human fat contains only a small fraction of thermogenic adipocytes which are scattered in broad regions [11, 12]. Positron emission tomography-computed tomography (PET-CT) scans have allowed the discovery of thermogenic fat cells in supraclavicular and neck region by measuring radiolabeled glucose uptake [13, 14], but have a limited sensitivity in the identification of tiny fractions. Besides, the abundance of thermogenic fat regresses during aging, weight gain and metabolic disorders in adult humans [12, 14, 15]. Currently, a number of signature genes, such as *UCP1*, *PRDM16* and *PPARGC1A*, have been proposed for identification of human adipose browning process [2, 3, 11]. However, these genes only been used to make a qualitative distinction, and have not been fully validated in human samples. Indeed, some of these genes have been proven to be weak classifiers in distinction of human adipose types.

Machine learning provide promising methods for quantifying human adipose browning. However, to construct a robust supervised learning model, hundreds of labeled adipose samples are required to train the algorithm. Unfortunately, neither considerable human brown-like fat samples nor well-established detection methods for human adipose browning are available. Deep learning methods, such as autoencoders, are able to summarize the biology features from unlabeled high-dimensional data, which provide an alternative way to obtain adequate human brown-like samples for supervised machine learning.

In this study, we developed two computational tools, which we call human browning capacity index (HBI) and absolute HBI (absHBI), for estimating the degree of browning

and quantifying the thermogenic potential of human fats based on high-throughput sequencing data. First, we defined robust molecular signatures of human thermogenic fats using experimental approaches and publicly available molecular profiles from various human brown-like adipocytes and adipose tissues. Next, we analyzed and isolated the indicator reflecting browning potential in training cohort using autoencoders. Using ensemble machine learning models, we constructed HBI and absHBI based on the expression levels and relative expression rankings (RERs) of signature genes, respectively. HBI was designed to predict the degree of browning and thermogenic potential in human pre-adipocytes, adipocytes and adipose tissues. absHBI was used to predict the adipose browning independent to control samples and without removing the batch effects. Importantly, both HBI and absHBI reflected browning degree, insulin sensitivity and glucose-lipid metabolic activity of human fats derived from obesity and type 2 diabetes mellitus (T2DM) patients.

Methods

Data acquisition

Publicly available microarray and RNA-sequencing cohorts used in this study were listed in Additional file 7: Table S1. For each study, batch effects were removed using ComBat function, which employs an empirical Bayes framework within the sva (version 3.40.0) R package. The gene names were mapped from any other formats to Human Genome Organization (HUGO) and eliminated genes without such mapping to ensure compatibility. Only protein coding genes were included in this analysis. If multiple probes shared the same symbol gene name, we calculated the mean of the expression values of these probes as the final expression value of the gene.

Identification of human brown-like fat signature genes

GSE56633 (BC1, n = 6), GSE57896 (BC2, n = 24), GSE71293 (BC3, n = 12), GSE125331 (BC4, n = 5), GSE113764 (BT1, n = 30) and GSE122721 (BT2, n = 6) datasets were used to identify human brown-like fat signature (HB) genes. Considering the batch effects, we performed DEGs analysis to these datasets respectively. For microarray data, DEGs analysis was performed by limma (version 3.48.3) R package [16], while DEGs analysis for RNA-seq datasets was conducted by DESeq2 (version 1.32.0) R package [17]. Genes consistently up-regulated in human brown-like fats in RobustRankAggreg (version 1.2) analysis were considered as the candidates of signature genes.

Experimental validation of human brown-like fat signature genes

Human tissue and cell culture

Human subcutaneous adipose tissues (SATs) from 3 healthy donors were obtained from Nanjing Drum Tower Hospital (Nanjing, China) after informed consent was obtained. For explant culture, adipose tissues were minced into small fragments (5–10 mg), and placed in M199 medium supplemented with 10% fetal bovine serum (FBS), 850 nM insulin and 5 μM dexamethasone (Dex) without or with rosiglitazone (1 μM) or creatine (5 mM). After 4 days in culture, the tissues were harvested for gene expression analysis. For cell culture, adipose-derived stem/stromal cells (ADSCs) were isolated from adipose tissue specimens by collagenase digestion (5 mg/mL type 1), and placed in MEM-α medium supplemented with 10%

FBS. All media were supplemented with 100 U/mL penicillin, 100 μg/mL streptomycin, and maintained in a humidified incubator at 37 °C under 5% CO_2.

Primary adipocyte differentiation

To generate human white adipocytes in vitro, ADSCs were seeded at a density of 2×10^4 cells per cm^2 and grown to confluency over ~ 5 days. White adipocytes differentiation was performed using differentiation medium for 14 days, and maintained in maintenance medium for 4 days. To induce human brown-like adipocytes, white adipocytes were treated with 1 μM rosiglitazone or 5 mM creatine for 4 days. All media were refreshed every 2 days. Finally, the adipocytes were harvested for gene expression analysis. The differentiation medium was comprised of DMEM/F-12 supplemented with 10% FBS, 850 nM insulin, 0.5 mM isobutylmethylxanthine (IBMX), 5 μM Dex, and 125 nM indomethacin (Indo), 1 nM triiodothyronine (T3). The maintenance medium was comprised of DMEM/F-12 supplemented with 10% FBS, 850 nM insulin and 1 nM T3. All media were supplemented with 100 U/mL penicillin, 100 μg/mL streptomycin, and maintained in a humidified incubator at 37 °C under 5% CO_2.

Quantitative real-time PCR

Total RNA was isolated from adipose tissues or adipocytes using TRIzol reagent (ThermoFisher), and cDNA was synthesized using a 5 × All-In-One RT MasterMix (abm, G486) kit according to the manufacturer's instructions. Quantitative real-time PCR (RT-qPCR) was performed on a StepOnePlus (Applied Biosystems) using AceQ qPCR SYBR Green Master Mix (Vazyme, Q111-02). The expression of the measured genes was normalized to the *RPLP0* mRNA expression levels. The sequences of the primers used in this study are shown in Additional file 8: Table S2. Statistical analysis was performed using GraphPad Prism software (version 8.0). Error bars indicated the Standard Error of Mean (SEM).

Experimental validation of brown-like fat signature genes in mice

C57BL/6 J mice (6–8 weeks old) were purchased from the Model Animal Research Center of the Nanjing University (Nanjing, China) and bred in the animal facilities under specific pathogen-free conditions. All mouse procedures and experiments for this study were approved by Institutional Animal Care and Use Committee, Nanjing University. Mouse white and brown adipose tissues were isolated for gene expression analysis from inguinal and interscapular region, respectively. We mapped HB gene IDs to mouse ortholog gene IDs to design primers for RT-qPCR analysis. The expression of the measured genes was normalized to the *Rplp0* mRNA expression levels. Statistical analysis was performed using GraphPad Prism software (version 8.0). Error bars indicated the Standard Error of Mean (SEM).

Prediction of the browning levels of human adipose samples by ensemble machine learning

Unsupervised machine learning

We adopted unsupervised deep learning method to look for the browning potential of SATs in GTEx cohort (n = 663). We normalized the raw counts of the RNA-seq samples using DESeq2 (version 1.32.0) R package [17] and performed autoencoders analysis by

keras (version 2.9.0) R package. We used mean squared error (MSE) as the loss function, and the optimizer is "adam". Mean absolute error (MAE) was used to monitor training of autoencoders. The training process was run for 30 epochs. Parallelly, the transcription factor activities in each sample were inferred by dorothea (version 1.4.1) R package [18]. The immune cells infiltration was evaluated via a deconvolution approach using R-based version of CIBERSORT [19]. The inflammatory response was estimated by single sample gene set enrichment analysis (ssGSEA) algorithm using GSVA (version 1.40.1) R package [20] with established gene lists of Molecular Signatures Database (version 7.3). The feature constructed by encoders which shows strong positive correlation to PPAR family transcription factor activities and negative association with proinflammatory immune cells infiltration and immune response was used to indicate the browning capacity of GTEx SAT samples. Based on the levels of selected encoder feature, we further filtered the HB genes which reflect the changes of browning levels using correlation analysis.

Establishment of human browning capacity index

We constructed a computational tool, which we call HBI (human browning capacity index), using ensemble method for quantifying the browning levels of human fats (Fig. 4A). SAT samples of GTEx cohort were randomly assigned to training and testing sets with a 7:3 ratio. In training set, we fitted machine learning models using the filtered HB genes as the covariates. The models included elastic net (ENET), random forest (RF), artificial neural networks (ANNs), and Bayesian regularized neural networks (BNNs). ENET is a regularized regression model that uses both L1-norm and L2-norm to penalize the coefficients in a regression model. RF is an ensemble algorithm that combines multiple decision trees using bagging method to increase the overall result. ANNs is a computational model that uses node layers to translate a data input into a desired output. BNNs is a robust machine learning model which reduces the need for cross-validation and offers principled uncertainty estimates from deep learning architectures. Hyperparameters of ENET, RF and ANNs were optimized using tenfold cross-validation in the training set to maximize the goodness of fit (R^2). The outputs of RF, ANNs and BNNs are stacked together and used as input to a generalized linear model to devise an ensemble model. This final estimator is trained through tenfold cross-validation. These models were all implemented using caretEnsemble (version 2.0.1) R package.

Validation of human browning capacity index

The performance of HBI in quantifying the browning levels were assessed in testing set and external human adipocyte and adipose tissue datasets. Furthermore, we compared the performance of HBI and traditional beige markers in estimating the degree of browning by meta-analysis. Random-effects meta-analysis model was used to calculate a standard mean difference (SMD). Genes ($SMD > 0$ & Overall $P \leq 0.05$) were considered as robust indices for quantifying the degree of browning.

Establishment and validation of absolute human browning capacity index

Absolute quantification tools based on relative expression ordering (REO) of genes have been shown to produce robust results in various applications such as cancer classification and stemness quantification [21, 22]. Inspired by REO method, we constructed

absolute HBI (absHBI) using relative expression ranking (RER) to intuitively evaluate the thermogenic potential of human fats (Fig. 6A). Firstly, using autoencoder F72 as an indicator of browning potential, we grouped GTEx SAT samples into high browning potential (high BP) group and low browning potential (low BP) group. For each sample, the rankings of *DHRS11*, *REEP6* and *STX11* and were obtained by ordering all the genes from low to high based on their expression levels. The rankings of the three HB genes are highly depended on the "background" genes used in the ordering process. Thus, we selected the background genes for ranking the three HB genes, respectively. Taking *DHRS11* as the example, the pairwise comparisons were performed for the expression level between *DHRS11* and all the other protein coding genes in all samples. Each gene pair (G_{DHRS11}, G_{other}) only has two possible REO outcomes (the gene expression of $G_{other} > G_{DHRS11}$ or $G_{other} < G_{DHRS11}$). We obtained the genes with certain REO ($G_{other} < G_{DHRS11}$) in half of the high BP samples but reversed REO ($G_{other} > G_{DHRS11}$) in at least half of the low BP samples. Then the correlation between *DHRS11* and background genes was analysis. Only genes showed negative association with the expression levels of *DHRS11* were used as background genes. Next, we reordered the signature genes against the background genes to obtain RER. The machine learning models were trained using the RERs of the signature genes as the covariates. The performances of absHBI in quantifying the browning potential were assessed using white and brown-like adipose samples in different datasets without removing the batch effects.

Statistical analysis

Statistical analysis was carried out using R (version 4.1.2) unless otherwise indicated. Differences were analyzed by unpaired Student's t test or one-way ANOVA depending on experimental conditions. $P \leq 0.05$ were considered statistically significant. Plots were generated using ggplot2 (version 3.3.5), ggpubr (version 0.4.0), ggtree (version 3.0.2), pheatmap (version 1.0.12), factoextra (version 1.0.7) R packages.

Results

Isolation and validation of signature genes for identification of human brown-like fats

We designed a bioinformatic pipeline which incorporated machine learning, deep learning and experimental analysis to construct robust metrics for quantifying browning degree of human fats (Fig. 1). Firstly, we isolated unbiased signature genes for identifying browning process in human fats. To achieve this goal, we systematically retrieved publicly available transcriptomes on differentiated adipocytes and adipose tissues from the microarray and RNA-seq studies of GEO databases (Fig. 2A). A total of 24 microarray samples and 59 RNA-seq samples, comprised high quality transcriptomic samples of human white and brown-like fat (Additional file 1: Fig. S1), were selected for downstream analysis. It contains a variety of experimental models for obtaining human brown-like fat specimens: Kishida et al. (BC1) induced human beige adipocytes from iPSCs or human dermal fibroblasts overexpressed *CEBPB* and *MYC* [23]. Moisan et al. (BC2) induced human beige adipocytes from human embryonic stem cells [24]. Barquissau et al. (BC3) and Singh et al. (BC4) induced human beige adipocytes from human mesenchymal stem cells via different induction strategies [25, 26]. Mueez et al. (BT1)

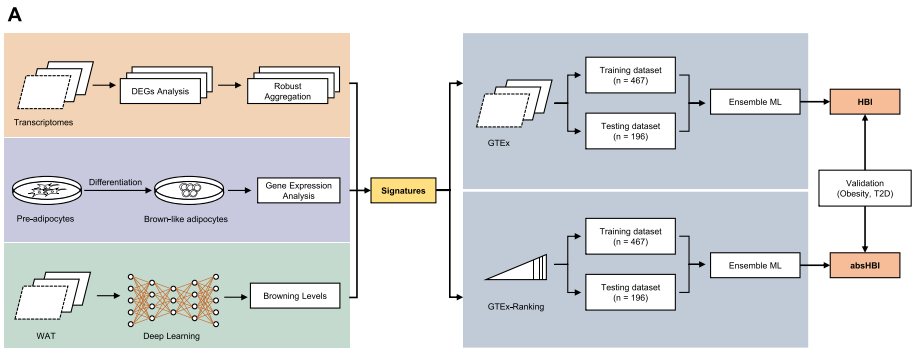

Fig. 1 Flowchart of the present study. **A** Flowchart showing methodology used to estimate the thermogenic potential of human fats. Human brown-like fat transcriptomes, WAT transcriptomes and primary adipocyte induction model are integrated to identify human browning signatures. Ensemble machine learning (ML) is applied to construct HBI and absHBI for browning detection

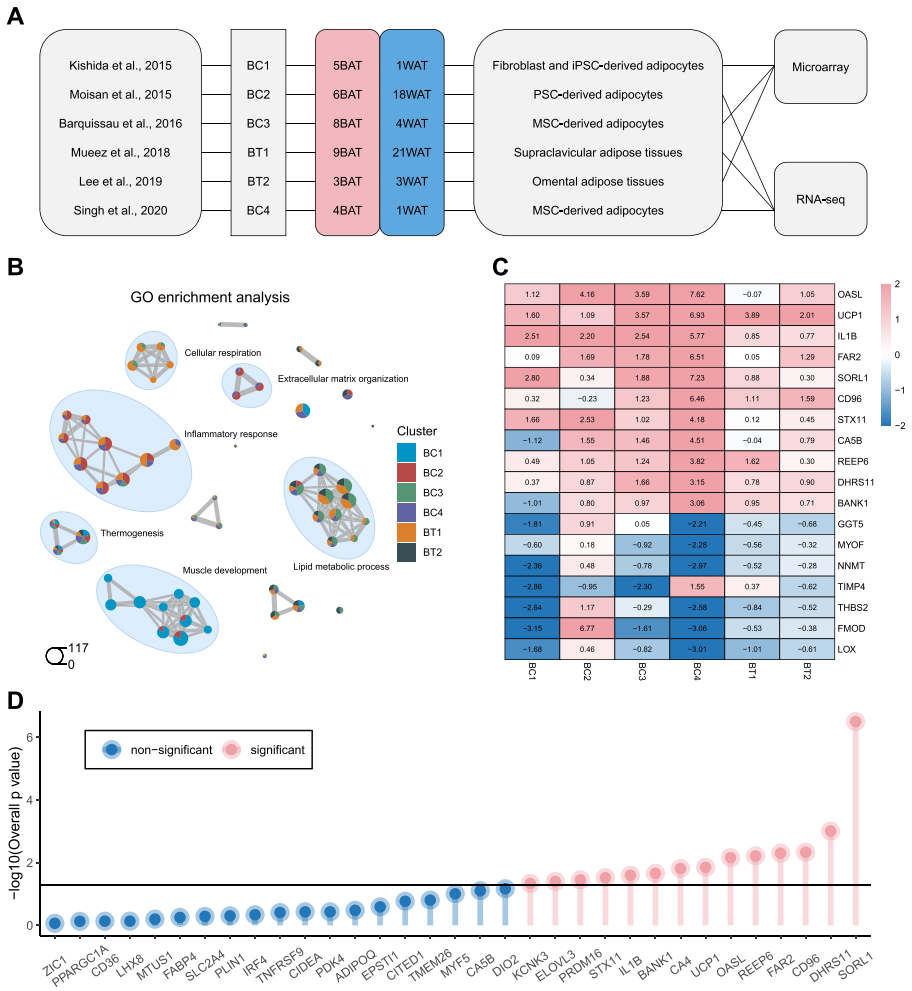

Fig. 2 Identification of signature genes of human brown-like fats. **A** Summary of the datasets used in the identification of signature genes of human brown-like fat. The number of samples, brief description and study type are indicated. **B** Semantic similarity between GO terms, the pie charts indicate highly enriched GO terms in the up-regulated genes of different datasets, the size of the pie indicates the number of enriched genes. **C** Heatmap showing the significantly up-regulated and down-regulated genes in different datasets. **D** Overall p values of meta-analysis with continuous outcome data using different genes

isolated thermogenic adipose tissues from supraclavicular region [27]. Lee et al. (BT2) induced thermogenic adipose tissues ex vivo from white adipose tissues (WATs) [28].

We performed differential expressed genes (DEGs) analyses to these datasets, respectively. We executed GO and KEGG enrichment analysis, to evaluate the biological similarity of these brown-like fats. The semantic similarity of significantly enriched terms was measured based on the annotation statistics of their common ancestor terms. By this means, we observed functional difference in these samples (Fig. 2B; Additional file 2: Fig. S2). The brown-like fats in BC3, 4 and BT1, 2 exhibited strong lipid metabolic activity. BC1 increased genes of muscle development. BC2 showed higher inflammatory response levels. In addition, BT1 exhibited stronger thermogenesis activity than the other cohorts, evidenced by enriched cellular respiration and thermogenesis related genes. These differences might result from individual and anatomical location difference, as well as technical variation, which may affect the performance of browning detection methods based on biological process distinctions.

We treated genes consistently up-regulated in brown-like fats from these cohorts as candidate genes for detecting browning process. We found 11 genes, including *OASL*, *UCP1*, *IL1B*, *FAR2*, *SORL1*, *CD96*, *STX11*, *CA5B*, *REEP6*, *DHRS11*, *BANK*, were robustly up-regulated in human brown-like fats using robust rank aggregation method (Fig. 2C). To evaluate the performance of these candidates in identification of browning process, we applied meta-analysis to these genes with previously used brown marker genes, including *ADIPOQ*, *CA4*, *CD36*, *CIDEA*, *CITED1*, *DIO2*, *ELOVL3*, *EPSTI1*, *FABP4*, *HOXC9*, *IRF4*, *KCNK3*, *LHX8*, *MTUS1*, *MYF5*, *PDK4*, *PLIN1*, *PPARG*, *PPARGC1A*, *PRDM16*, *SHOX2*, *SLC2A4*, *TMEM26*, *TNFRSF9*, *UCP1* and *ZIC1* [26, 29–31]. UCP1 is a shared gene in both candidate and traditional gene list. We found that 10/11 candidate genes, including *OASL*, *UCP1*, *IL1B*, *FAR2*, *SORL1*, *CD96*, *STX11*, *REEP6*, *DHRS11*, *BANK*, were informative in qualitative distinction of browning process, which highlighted the applicable of our pipeline in human browning signature selection. However, among the pool of 26 conventional markers, only 4 genes (*KCNK3*, *ELOVL3*, *PRDM16* and *CA4*) exhibited a modest level of significance in relation to human brown-like fats (Fig. 2D; Additional file 3: Fig. S3). Moreover, the levels of classical markers, such as *UCP1*, was not always associating to the degree of browning (Additional file 3: Fig. S3). This result was consistent with previous reports that *UCP1* was a weak classifier for analyzing human brown-like adipose biopsies [11, 32].

Deep learning reveals browning degree and signature genes of human brown-like adipose samples

To qualify the adipose browning degrees, we further selected the signature genes highly associated with browning levels of human adipose samples, from the genes which were qualified for qualitative distinction of browning process. To achieve this goal and further machine learning task, considerable human brown-like adipose samples is required. However, human fat contains only a small fraction of thermogenic adipocytes which are scattered in broad regions. There are also lack of efficient clinical induction and detection methods for human adipose browning. These obstacles limited the sampling of human brown-like fats. Nonetheless, taking advantage of the wealth of data on global transcriptomic studies of fat depots published over the last decade, we obtained

adequate unlabeled human fat RNA-seq samples from several human studies, such as Genotype-Tissue Expression (GTEx) cohort. GTEx cohort provides high-quality WAT gene expression information from individuals with different age, gender and health status. These discrepancies lead to the alterations of browning levels, which would be captured by deep learning models. Thus, we performed dimension reduction using autoencoders, which summarized the transcriptional features of GTEx SAT samples to 100 features (Fig. 3A). These indices reflected the primary characteristics of GTEx SAT samples. By enrichment analysis, we observed that feature 72 (F72) showed positive association (R = 0.67) with GO term "Thermogenesis" (Fig. 3B, C), suggesting that the levels of F72 may reflect the browning capacity of these samples. Considering that the browning level of adipose tissues is highly associated to their lipid metabolic activities [33], we further evaluated the fatty acid (FA) biosynthesis and degradation activity by single sample gene set enrichment analysis (ssGSEA) algorithm. The transcriptional activities of PPAR family proteins, including PPARα, PPARδ, PPARγ, which dominated the lipid metabolism in adipocytes [12], were inferred by an integrative method, called DoRothEA [18]. We noted that high F72 was associated with higher activities of FA biosynthesis and degradation as well as higher PPARα, PPARδ, PPARγ transcriptional activities (Fig. 3D).

Furthermore, previous reports demonstrated that the crosstalk between adipocytes and immune cells was important to thermogenic activation [2, 12]. For instance, M1-like macrophages produce pro-inflammatory cytokines such as TNFα and IL-1β to impair the thermogenetic capacity of adipose tissues. Conversely, anti-inflammatory M2-like macrophages produce cytokines such as IL-4 and IL-10, which promote brown fat activation and beige adipose tissue remodeling. Thus, we evaluated immune cell types for their relative abundance in adipose tissue microenvironment by CIBERSORT. In addition to individual immune subpopulation fractions, we also considered the functional activation of immune cells by measuring the intensity of inflammatory signaling. The results revealed that SATs in high F72 group showed higher score of M2-like macrophages infiltration and lower levels of M1-like macrophages infiltration (Fig. 3F), suggesting that the niche of F72 high WATs supported beige cells biogenesis. Consistent with this finding, F72 was negatively correlated to the activities of TNFα (R = − 0.51), IFNα (R = -0.5) and IFNγ (R = − 0.52) pathway (Fig. 3E). As a consequence, the levels of F72 were informative in human adipose browning prediction.

Using F72 as an indicator of browning capacity, we investigated the expression alterations of the signature genes in white adipose tissues. Notably, we found that only *BANK1* (R = 0.74), *DHRS11* (R = 0.49), *REEP6* (R = 0.7) and *STX11* (R = 0.47) showed strong positive correlation with F72 (Fig. 3G), while the expression levels of *OASL*, *UCP1*, *IL1B*, *FAR2*, *SORL1* and *CD96* exhibited no or negative association to F72 (Additional file 4: Fig. S4). Thus, *BANK1*, *STX11*, *REEP6* and *DHRS11* were adopted to quantify browning levels of human adipose tissues.

Experimental validation of the signature genes using human and mouse adipose samples

To provide a more stringent validation to *BANK1*, *DHRS11*, *REEP6* and *STX11*, we validate their availability in experimental analysis (Fig. 4A). We first investigated their expressions in primary cell cultures derived from human white adipose tissues. We

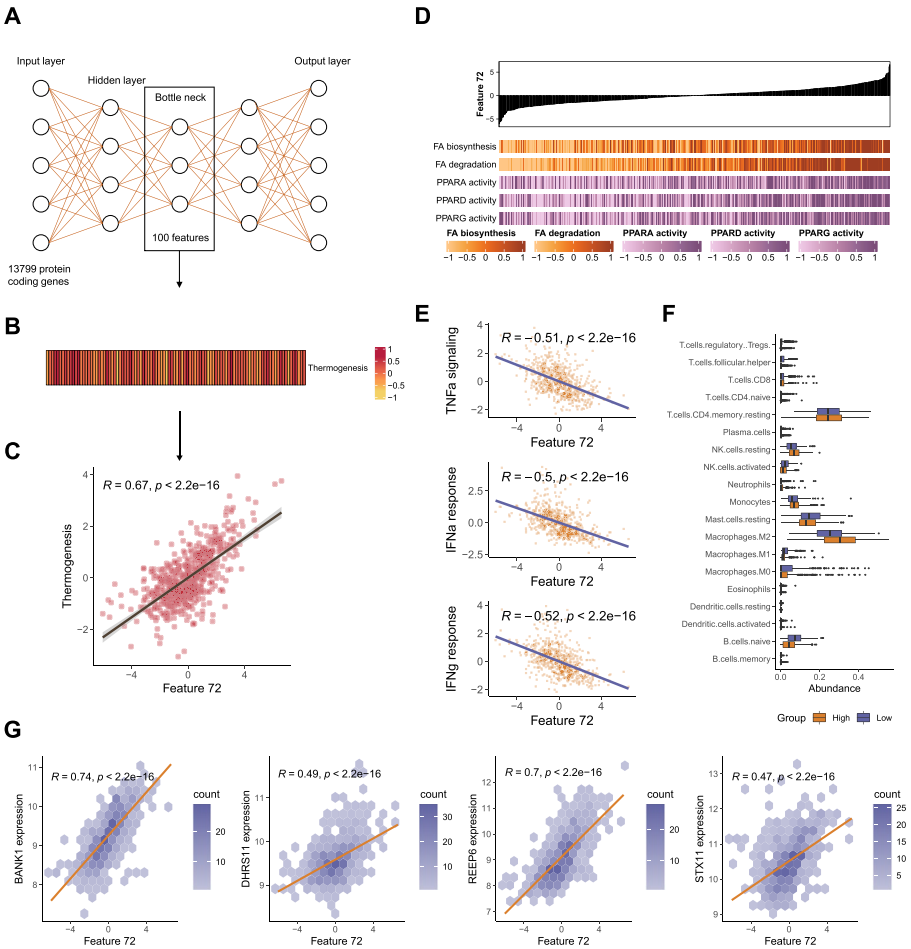

Fig. 3 Deep learning reveals browning degree and signature genes of human brown-like fats. **A** An autoencoder model for interpreting human adipose samples. **B** Heatmap showing the correlation between the autoencoder features of GO term "Thermogenesis". **C** Correlation between the autoencoder feature 72 (F72) and GO term "Thermogenesis" (n = 663). **D** Overviews of the association between biological features and F72 (n = 663). Columns represent samples sorted by F72 levels from low to high. Rows represent molecular and biological processes associated with F72, including fatty acid (FA) biosynthesis, FA degradation, PPARα activity, PPARβ activity and PPARγ activity. **E** Correlation between F72 levels and z-scored ssGSEA scores of inflammation-related pathway activity (n = 663). **F** Relative abundance of indicated immune cell types in F72 high group and low group (n = 663). **G** Correlation between F72 levels and the expression levels of the signature genes (n = 663)

isolate CD34- CD45- CD44 + CD90 + CD105 + mesenchymal stem/progenitor cell (Fig. 4B). The classical white adipocytes browning process was induced by PPARγ agonists rosiglitazone as the pipeline showed (Fig. 4A). The expression levels of the signature genes were measured by real-time quantitative PCR (RT-qPCR). These methods have been widely used in adipose browning detection. The result showed that the beige adipocytes significantly up-regulated these signature genes except for *BANK1* (Fig. 4C). Thus, we excluded *BANK1* in further analysis. To simulate to adipose browning process in vivo, we performed ex vivo explant cultures. As expected, rosiglitazone also promoted *DHRS11*, *REEP6* and *STX11* expression in human adipose tissues (Fig. 4D). Intriguingly, we found the levels of the three signature genes also increased in creatine-induced thermogenic cells and tissues (Fig. 4E), suggesting

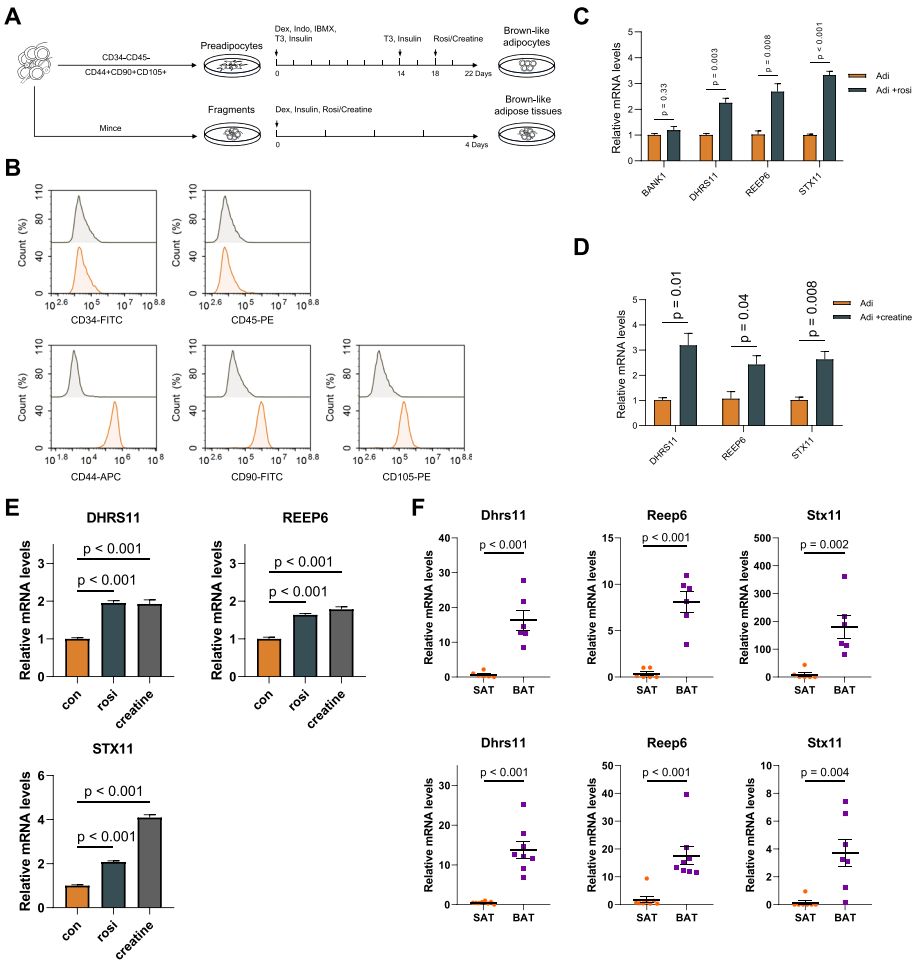

Fig. 4 Experimental validation of the signature genes in human and mouse samples. **A** Schematic illustration of experimental design. **B** Cell surface marker identification of human mesenchymal stem/progenitor cells. **C** RT-qPCR validation of the signature genes in white and rosiglitazone (rosi) induced human brown-like adipocytes (n = 3 biological replicates). **D** RT-qPCR validation of the signature genes in human white and creatine induced brown-like adipocytes (n = 3 biological replicates). **E** RT-qPCR validation of the signature genes in brown-like adipose tissues from healthy donors (n = 3 biological replicates). **F** RT-qPCR validation of the signature genes in female (upper, n = 12) and male (lower, n = 16) mouse adipose tissues. Differences were analyzed by unpaired Student's t test. Error bars indicated the SEM

that these genes were suitable for the identification of UCP1-independent thermogenesis. Furthermore, mouse has been the most widely used model animal for adipose biology study, however, recent study highlighted the contrasts between human and mouse brown-like adipocytes [29, 34]. Universal markers for browning detection will increase the interpretability of results from mouse models. Thus, we investigated the expression changes of the three signature genes in mouse adipose tissues using their ortholog genes. Consistent with human samples, the expression levels of *Dhrs11*, *Reep6* and *Stx11* were markedly up-regulated in mouse brown adipose tissues (BATs), suggesting the applicability of these genes in mouse model (Fig. 4F). Together, we proposed *DHRS11*, *REEP6* and *STX11* as the signature genes for identification and quantification of human browning process. Dehydrogenase/reductase member 11

(DHRS11) is a type of 17β-hydroxysteroid dehydrogenase which is involved in steroid biosynthetic process. Receptor accessory protein 6 (REEP6) plays a role in regulating endoplasmic reticulum (ER) membrane structure. ER is indispensable for brown adipocytes mitochondrial dynamics and function [35]. Syntaxin 11 (STX11) is a member of the SNARE protein family, which has been implicated in the lipid metabolism by binding to adipose-triglyceride-lipase (ATGL) [36].

Prediction of human adipose browning capacity by machine learning

Take advantage of the expression levels of *DHRS11*, *REEP6* and *STX11* and the output of autoencoders, we constructed a prediction model for evaluating human adipose browning processes. The adipose samples of GTEx dataset were randomly assigned to training and testing sets with a 7:3 ratio. For model selection, we fitted regression models using *DHRS11*, *REEP6* and *STX11* as the covariates with the training set (Fig. 5A). These models included elastic net (ENET), random forest (RF), artificial neural networks (ANNs), and Bayesian regularized neural networks (BNNs), as well as an ensemble model stacking the outputs of above-mentioned models using generalized linear model.

The performances of different models were assessed in testing set and independent studies. The ensemble model exhibited highest accuracy at evaluating the browning degrees of adipose samples from training ($R = 0.82$) and testing ($R = 0.72$) sets (Fig. 5B). This model also correctly predicted the levels of browning in adipocyte ($p = 0.028$) and adipose tissue ($p = 0.035$) samples (Fig. 5B). Therefore, we employed the ensemble model to calculate human adipose browning index (HBI). To validate the performance of HBI in the identification of browning process, we grouped the fat samples into HBI high and low group according to the mean of HBI and conducted single sample gene set enrichment analysis (ssGSEA). As shown in Fig. 5C, WAT samples with high HBI exhibited brown-like phenotypes, such as increased lipid metabolism, PPAR pathway and AMPK pathway activity. Notably, HBI high samples also enriched genes involving in insulin pathway activity, indicating that the HBI levels reflected the insulin sensitivity of adipose tissues. Furthermore, we found that HBI was robust to the estimation of browning potential in human fat datasets and increased across all studies using meta-analysis (Fig. 5D, E). In conclusion, HBI was robust to the identification and quantification of browning levels in various types of adipose samples.

HBI is highly correlated with adipose browning capacity in obesity and type 2 diabetes mellitus patients

Obesity and metabolic disorders such as type 2 diabetes mellitus (T2DM) impair the browning capacity of white adipose tissues. We examined adipose samples of obesity and T2DM patients to investigate whether the HBI predict browning capacity in these adipose tissues. Although modestly decreased, the HBI showed positive correlation to the thermogenesis ($R_{overweight} = 0.49$, $R_{obese} = 0.36$) and FA degradation ($R_{overweight} = 0.5$, $R_{obese} = 0.39$) in adipose tissues from overweight and obesity individuals (Fig. 6A). Consistently, high HBI levels were strongly associated with higher expressions of lipid metabolism related genes, such as *FASN*, *CPT2*, *COX5A*, *COX6A1* and *PPARG* (Fig. 6B). These results were further validated by enrichment analysis, which showed significant enrichment of lipid metabolism, thermogenesis and insulin response associated genes

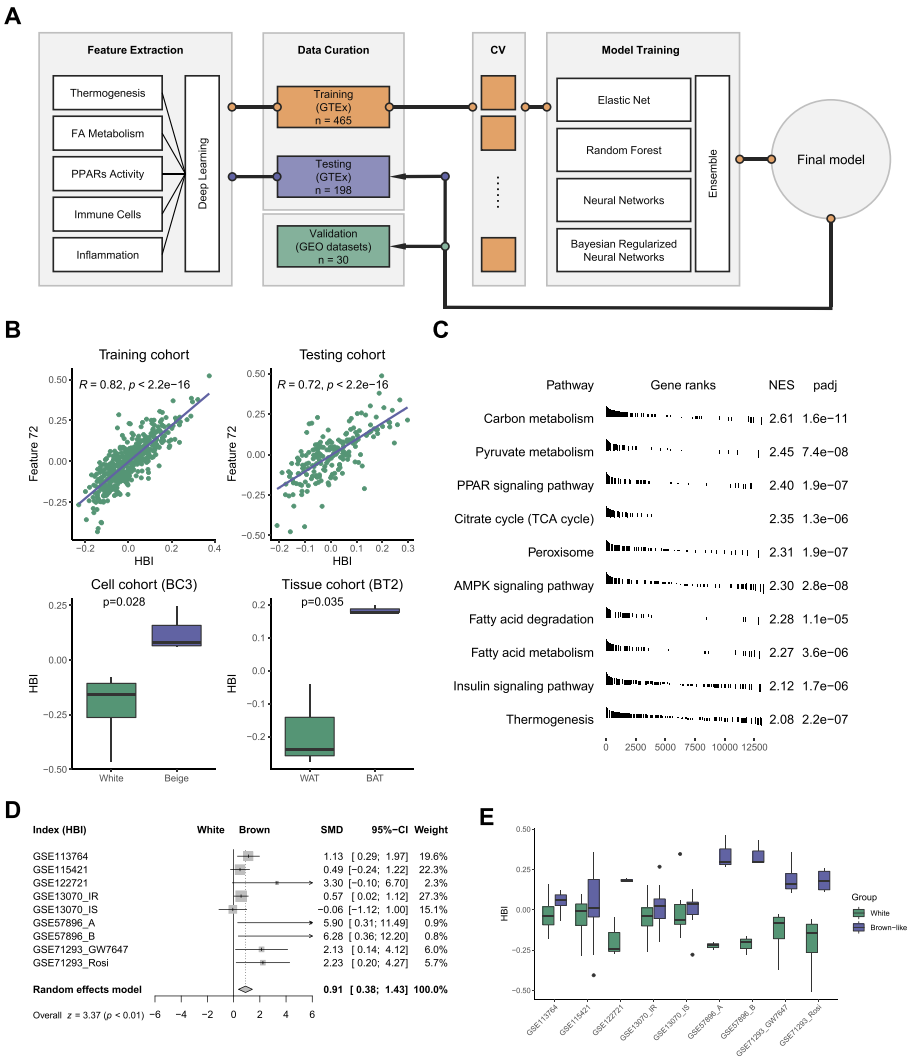

Fig. 5 Prediction of browning capacity using ensemble machine learning model. **A** Pipeline for the prediction of adipose browning capacity using ensemble machine learning model. **B** Correlation between human browning capacity index (HBI) and F72 levels in WAT training cohort (n = 467), WAT testing cohort (n = 196), brown-like adipocyte validation cohort (n = 12) and tissue validation cohort (n = 6). **C** GSEA analysis predicting that high HBI is positively correlated with thermogenesis potential in the training cohort. **D** Forest plots showing performance of HBI in the classification of thermogenesis related processes. **E** Levels of HBI in different human brown-like datasets, samples were grouped into white and brown-like adipose groups

in HBI high fats of overweight and obese patients (Fig. 6C). Moreover, we validated the performance of HBI in the evaluation of the browning capacity in adipose tissues of insulin resistance (IR) patients. As expected, the HBI successfully quantified the degree of browning in IR patients (Fig. 6D–F), suggesting that HBI reflected the lipid metabolic activity and insulin sensitivity in T2DM patients.

Development of absolute human adipose browning capacity index

Inspired by relative expression ordering (REO) method, we developed an absolute HBI (absHBI) for intuitively evaluating the browning degree and potential of human fats in response to the various stimuli without the assistance of control groups

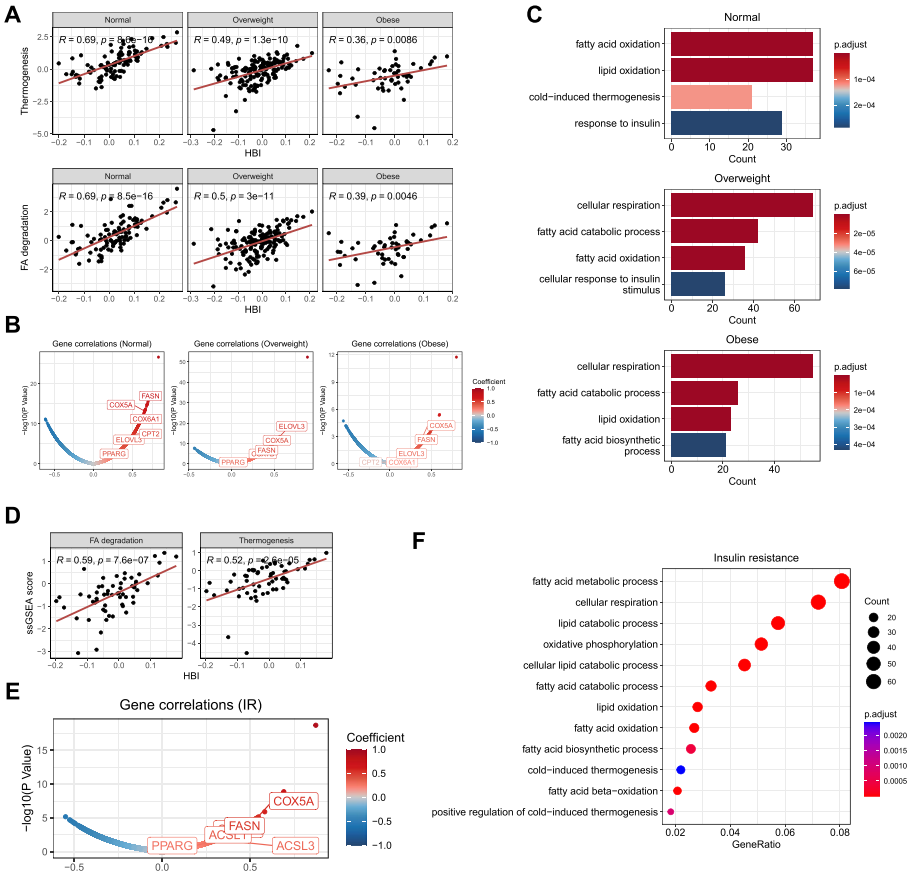

Fig. 6 Performance of HBI in the quantification of browning potential in obesity and T2DM patients. **A** Correlation between HBI and z-scored ssGSEA scores of Thermogenesis and FA degradation in normal (n = 102), overweight (n = 153) and obese (n = 51) individuals. **B** Volcano plot showing the Pearson coefficients between HBI and genome-wide (n_{gene} = 13,530) gene expression levels in normal (n = 102), overweight (n = 153) and obese (n = 51) group. Several lipid metabolism-related genes are annotated on the plot. **C** GO enrichment analysis to the genes that positively correlated to HBI levels in normal, overweight and obese individuals. **D** Correlation between HBI and z-scored ssGSEA scores of Thermogenesis and FA degradation in insulin resistance (IR) patients (n = 59). **E** Volcano plot showing the Pearson coefficients between HBI and genome-wide gene expression levels in IR group. Several lipid metabolism-related genes are annotated on the plot. **F** GO enrichment analysis to the genes that positively correlated to HBI levels in IR patients

(Fig. 7A). Firstly, we arranged the genes in every single GTEx SAT samples according to their expression levels. We observed that the rankings of the three signature genes (*DHRS11*, *REEP6* and *STX11*) exhibited positive correlation to the F72 levels (Fig. 7B), indicating that the rankings of the three signature genes in RNA-seq study also reflected the browning potential of human fats. Obviously, the rankings of a selected genes are highly depended on the "background" genes used in the ordering process. To highlight the alterations of the signature genes, we selected the background genes which are negatively correlated to the rankings of signature genes, we further filtered the genes with certain REOs. Finally, we obtained 132, 335, 274 background genes for *DHRS11*, *REEP6* and *STX11* respectively. Using these genes as background genes, we

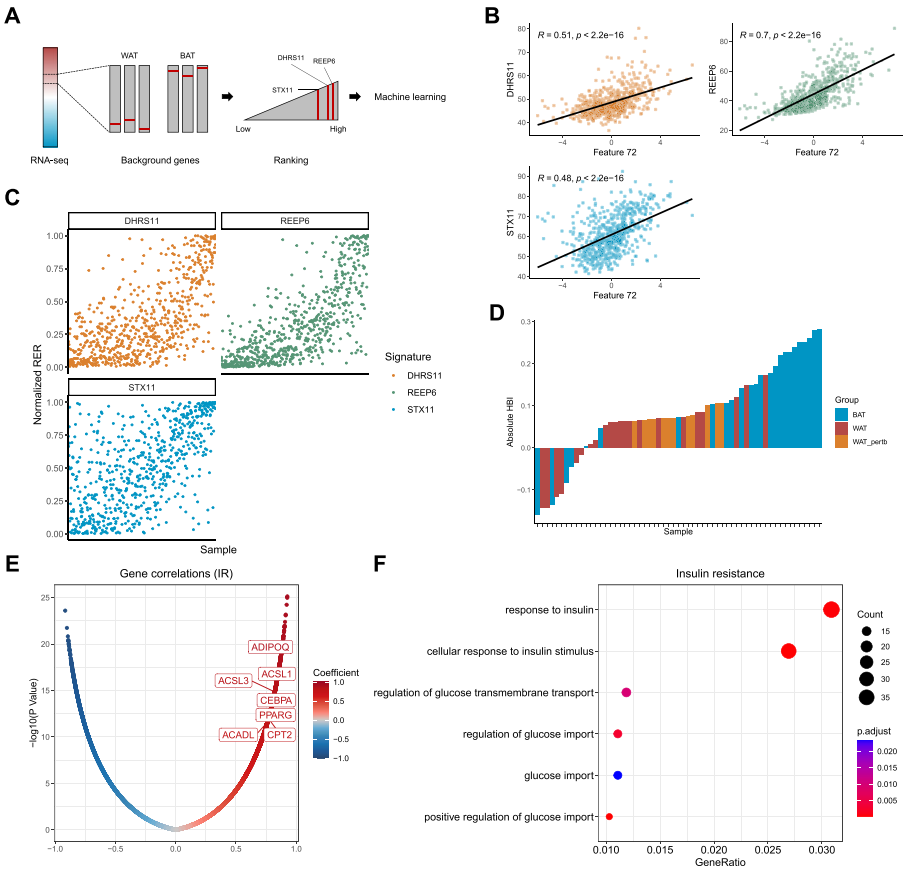

Fig. 7 Development and validation of absolute human browning capacity index. **A** Pipeline for the development of absolute HBI (absHBI) using machine learning. **B** Correlations between the rankings of *DHRS11*, *REEP6* and *STX11* and F72 (n = 663). **C** Normalized relative expression rankings (RERs) of signature genes (n = 663). Samples are sorted by F72 levels from low to high. **D** The absHBI levels of white and brown-like fat samples (n = 59). WAT_pertb: WAT samples treated with known small molecules. **E** Volcano plot showing the Pearson coefficients between absHBI and genome-wide gene expression levels in IR group. **F** GO enrichment analysis to the genes that positively correlated to absHBI levels in IR patients

calculated the relative expression rankings (RERs) of the signature genes (Fig. 7C) and fit ensemble machine learning model to obtain absHBI.

To validate the performance of absHBI, we applied this computational model to three independent RNA-seq datasets without removing batch effects. As anticipated, we found that the absHBI was robust to the classification between white and brown-like adipose samples. Notably, we observed that the absHBI levels was perturbed mainly by treatment and individual difference instead of batch effects caused by technological and experimental variants (Fig. 7D), suggesting that the absHBI was highly robust against the batch effects and sample normalization and can be stably applied to independent datasets. By correlation and enrichment analysis, we found that high absHBI was positively correlated to insulin response and glucose import related genes and processes (Fig. 7E, F). Altogether, these results demonstrated that the absHBI can be applied to quantify browning potential in T2DM patients derived adipose samples. Last but not least, we compared the performance of our computational models and previously reported tool ProFAT in predication of the browning capacity in different types of human adipose

samples. HBI and absHBI exhibited higher accuracy in adipocyte and adipose tissue samples than ProFAT (Fig. 5B; Additional file 6 Fig. S6A). All the models were more informative to distinguish thermogenic fat from WATs (Additional file 6: Fig. S6B).

Discussion

Adipose tissue is an extraordinarily flexible organ, which dramatically alters the cellular size and composition in response to various stimuli, including nutritional states and temperatures [1]. These adaptative remodeling play a central role in the regulation of energy homeostasis, body temperature and immune responses [37]. A notable remodeling process that has drawn particular attention is the "browning" or "beiging" of white adipose tissue (WAT), in which mitochondria-enriched thermogenic fat cells with multilocular lipid droplets emerge within WAT. Current studies demonstrate that promoting WAT browning and BAT activation improves metabolic health in ways far beyond the induction of thermogenesis [5, 12]. For example, Maria et al. showed that cold exposure significantly increased energy expenditure, whole-body glucose disposal and insulin sensitivity [38]. Brian et al. used the mirabegron, a β3-adrenergic receptor agonist that stimulates beige cells formation in WAT, to improve glucose homeostasis in obese humans [39]. Such physiological and medical intervention provides promising therapeutic measures to the treatment of metabolic disorders. A robust quantification method for human brown-like fat recruitment therefore would predict clinical outcome and lead to the development of therapeutic measures that improve metabolic health. What is noteworthy is that most of previous studies quantified the degree of browning via PET-CT, a method that was commonly used to diagnose and stage cancers by measuring glucose uptake. However, PET-CT scans showed limited sensitivity in the identification of some adipose fractions. For instance, there is evidence that PET-CT scans failed to detected the glucose uptake in subcutaneous and visceral WAT depots after cold acclimation [40], while the other experimental study using RT-qPCR revealed that these adipose depots exhibited strong browning capacity in response to cold exposure [38, 39]. Thus, it is remains challenging in quantifying the browning potential on human fats. In the present study, we proposed signature genes and unbiased computational pipeline for evaluating the browning capacity of human fats. To the best of our knowledge, this is the first study in which human fat samples comprised of pre-adipocytes, adipocytes and adipose tissues have been leveraged to develop classification tools and machine-learning algorithm for analysis of human adipocyte browning. Importantly, these molecular metrics can evaluate the degree of browning for adipose samples derived from obesity and T2DM patients.

Previous studies analyzing gene expression patterns of brown-like adipocytes provided a number of signature genes for identification of adipose types [37]. However, most of the marker genes showed limited application because of experimental batch effects and data normalization biases. For instance, uncoupling protein 1 (UCP1) is a mitochondrial inner membrane protein that uncouple respiration and dissipate chemical energy as heat. The long-standing notion has been that UCP1 is the key driver of thermogenesis, which has been used as the classical marker gene of thermogenic adipocytes [41]. However, emerging evidence illustrates that UCP1 is insufficient to predict adipocyte types. As for human beings, the thermogenic potential of human fat does not always correlate

with the recruitment of UCP1-positive cells [11, 32]. Indeed, recent discoveries have highlighted several UCP1-independent thermogenic pathways in mammals [3]. Consequently, there are still lack of signature genes for identification of thermogenic adipocytes. In this article, we demonstrated that the three signature genes *DHRS11*, *REEP6* and *STX11* not only predicted the UCP1-dependent thermogenesis, but also exhibited powerful capacity in the identification of UCP1-independent thermogenesis. Thus, these genes have broad application in the browning characterization, while the generalizability of these genes is limited in predicting the heterogeneity of human thermogenic adipocytes. More studies using controlled trials and meta-analysis are needed to solve this issue.

T2DM is an expanding global health problem, closely linked to the metabolic disorder of adipose tissues [42]. Although the human browning index (HBI) we developed was robust to the quantitation of the adipose browning capacity in obesity and T2DM, an absolute index still needed to intuitively evaluate the degree of browning of adipose depots in response to the clinical treatment. we therefore developed absolute HBI (absHBI) based on the relative expression ordering (REO) which was used to quantify stemness [21]. To the best of our knowledge, this is the first study in which REOs have been employed to develop classification tools for analysis of human adipocyte browning. When applying absHBI to the adipose samples derived from insulin resistance individuals, we found that higher absHBI values were significantly relevant to the increased degree of browning in white adipose tissues, which showed the applicability of the absHBI in T2DM clinical investigation.

The present study has several strengths. First, our study proposed robust signature genes for identifying human thermogenic fats. We provided a stringent validation to the candidate genes using experimental approaches and publicly available molecular profiles from a spectrum of human adipose-related samples. The three signature genes, *DHRS11*, *REEP6* and *STX11*, turned out to be robust classifiers of human white and brown-like fats. Notably, these signature genes were also up-regulated in creatine-induced brown-like fat samples, which proved the applicability of these genes in UCP1-independent thermogenesis. Second, we applied the outcome of deep learning to train the supervised models, that provide an alternative way to quantify the thermogenic potential of human fats, which could be applied to other regression problem to train the machine learning model using unlabeled samples. Another important strength of our study was that we employed ensemble method for model construction, which outperformed any other separate conventional machine learning models. This method complements properties exhibited by single existing models and further augment the generalization capability.

Conclusions

In conclusion, we proposed *DHRS11*, *REEP6* and *STX11* as signature genes of human brown-like fats. Based on the expression patterns of these genes, we devise computational tools, named HBI and absHBI, for quantifying the browning degree and potential of human fats. HBI could be applied to control tests to distinguish human brown-like fats from white adipose samples. absHBI is developed to intuitively evaluate the thermogenic potential and enables the integration of adipose RNA-seq samples from different datasets. The findings based on our metrics may advance the

mechanism study for adipose-based targeted therapy for metabolic disorders such as T2DM, perhaps leading eventually to new targets that guide clinical diagnosis, or improve therapeutic effects.

Abbreviations

T2DM	Type 2 diabetes mellitus
PET-CT	Positron emission tomography-computed tomography
HBI	Human browning capacity index
absHBI	Absolute human browning capacity index
WAT	White adipose tissue
BAT	Brown adipose tissue
RER	Relative expression ranking
REO	Relative expression ordering
HB	Human brown-like fat signature
BP	Browning potential
SATs	Subcutaneous adipose tissues
ADSC	Adipose-derived stem/stromal cells
ENET	Elastic net
RF	Random forest
ANNs	Artificial neural networks
BNNs	Bayesian regularized neural networks
DEG	Differential expressed gene
ssGSEA	Single sample gene set enrichment analysis

Supplementary Information

The online version contains supplementary material available at https://doi.org/10.1186/s40537-024-00879-9.

Additional file 1: Figure S1. Unsupervised clustering to the human adipose datasets. **A** Principal component analysis (PCA) revealing the transcriptional difference between human and brown-like adipose samples in BC1 (n = 6), BC2 (n = 12), BC3 (n = 12), BC4 (n = 5), BT1 (n = 30) and BT2 (n = 6) datasets. *WAT* white adipose tissue, *BAT* brown-like adipose tissue.

Additional file 2: Figure S2. Semantic similarity of enrichment analysis in up-regulated genes. **A** Semantic similarity of KEGG terms. The pie charts indicate highly enriched terms in the up-regulated genes of different datasets, the size of the pie indicates the number of enriched genes.

Additional file 3: Figure S3. Gene expression levels of human brown-like marker genes. **A** Gene expression levels of indicated human brown-like adipose marker genes in different datasets. (*IR* insulin resistance, *IS* insulin sensitive, *Rosi* rosiglitazone).

Additional file 4: Figure S4. Correlations between F72 and browning marker genes in human adipose samples. **A** Correlation between the levels of autoencoder feature 72 and indicated marker genes. The Pearson coefficient (R) and p value are labeled in the plots.

Additional file 5: Figure S5. Performance of different machine learning algorithms in predication of browning capacity. **A** Performance of different machine learning algorithms in the adipocyte cohort BC3 (n = 12). **B** Performance of different machine learning algorithms in the adipose tissue cohort BT2 (n = 6). (*enet* elastic net, *rf* random forest, *brnn*: bayesian regularized neural networks)

Additional file 6: Figure S6. Performance of ProFAT in predication of human browning capacity. **A** Performance of ProFAT in the predication of human browning capacity in adipose tissues (BT2 dataset, n = 6) and adipocytes (BC3 dataset, n = 12). **B** Comparison of the performance of HBI, absHBI and ProFAT in the predication of browning capacity using GTEx SAT RNA-seq samples (n = 663).

Additional file 7: Table S1. Accession numbers of the transcriptomic profiles used in this article.

Additional file 8: Table S2. The sequences of the primers used in this article.

Additional file 9. The analysis code generated in the study.

Acknowledgements

We acknowledge GTEx and GEO database for providing their platforms and contributors for uploading their meaningful datasets.

Author contributions

YW and SZ performed the analyses and wrote the first draft of the paper. NY, AJ and WZ provided scientific suggestions and contributed to the manuscript revision. PS and ZH supervised the project and wrote the paper. All authors read and approved the final manuscript.

Funding
This work was supported by grants from the Guangdong Basic and Applied Basic Research Foundation (2021B1515120016), the Natural Science Foundation of Jiangsu Province (BK20222009), and the National Natural Science Foundation of China (82304492).

Availability of data and materials
All data used in this study are publicly available. Data from GTEx are available at https://gtexportal.org/. Data from the human study are available through the Gene Expression Omnibus (GEO). Data from the Molecular Signatures Database (MSigDB) are available at https://www.gsea-msigdb.org/gsea/msigdb. The codes generated or used during the study appear in the submitted article (Additional file 9). The codes for HBI and absHBI analysis are available at the GitHub repository (https://github.com/XiaoXxin/HBI). Any additional information required to reanalyze the data reported in this paper is available from the lead contact upon request.

Declarations

Ethics approval and consent to participate
Not applicable.

Consent for publication
Not applicable.

Competing interests
The authors declare that they have no competing interests.

Received: 2 October 2022 Accepted: 5 January 2024
Published online: 11 February 2024

References

1. Sakers A, De Siqueira MK, Seale P, et al. Adipose-tissue plasticity in health and disease. Cell. 2022;185(3):419–46. https://doi.org/10.1016/j.cell.2021.12.016.
2. Wang W, Seale P. Control of brown and beige fat development. Nat Rev Mol Cell Biol. 2016;17(11):691–702. https://doi.org/10.1038/nrm.2016.96.
3. Cohen P, Kajimura S. The cellular and functional complexity of thermogenic fat. Nat Rev Mol Cell Biol. 2021;22(6):393–409. https://doi.org/10.1038/s41580-021-00350-0.
4. van Marken Lichtenbelt WD, Vanhommerig JW, Smulders NM, et al. Cold-activated brown adipose tissue in healthy men. N Engl J Med. 2009;360(15):1500–8. https://doi.org/10.1056/NEJMoa0808718.
5. Becher T, Palanisamy S, Kramer DJ, et al. Brown adipose tissue is associated with cardiometabolic health. Nat Med. 2021;27(1):58–65. https://doi.org/10.1038/s41591-020-1126-7.
6. Hasegawa Y, Ikeda K, Chen Y, et al. Repression of adipose tissue fibrosis through a prdm16-gtf2ird1 complex improves systemic glucose homeostasis. Cell Metab. 2018;27(1):180-94.e6. https://doi.org/10.1016/j.cmet.2017.12.005.
7. Ikeda K, Kang Q, Yoneshiro T, et al. UCP1-independent signaling involving SERCA2b-mediated calcium cycling regulates beige fat thermogenesis and systemic glucose homeostasis. Nat Med. 2017;23(12):1454–65. https://doi.org/10.1038/nm.4429.
8. McDonald ME, Li C, Bian H, et al. Myocardin-related transcription factor A regulates conversion of progenitors to beige adipocytes. Cell. 2015;160(1–2):105–18. https://doi.org/10.1016/j.cell.2014.12.005.
9. Wang W, Chen J, Li M, et al. Numerical simulation of temperature and fluid fields in solidification process of ferritic stainless steel under vibration conditions. Crystals. 2019. https://doi.org/10.3390/cryst9030174.
10. Cohen P, Levy JD, Zhang Y, et al. Ablation of PRDM16 and beige adipose causes metabolic dysfunction and a subcutaneous to visceral fat switch. Cell. 2014;156(1–2):304–16. https://doi.org/10.1016/j.cell.2013.12.021.
11. Cheng Y, Jiang L, Keipert S, et al. Prediction of adipose browning capacity by systematic integration of transcriptional profiles. Cell Rep. 2018;23(10):3112–25. https://doi.org/10.1016/j.celrep.2018.05.021.
12. Rui L. Brown and beige adipose tissues in health and disease. Compr Physiol. 2017;7(4):1281–306. https://doi.org/10.1002/cphy.c170001.
13. Cohade C, Osman M, Pannu HK, et al. Uptake in supraclavicular area fat ("USA-Fat"): description on 18F-FDG PET/CT. J Nucl Med. 2003;44(2):170.
14. Cypess AM, Lehman S, Williams G, et al. Identification and importance of brown adipose tissue in adult humans. N Engl J Med. 2009;360(15):1509–17. https://doi.org/10.1056/NEJMoa0810780.
15. Berry DC, Jiang Y, Arpke RW, et al. Cellular aging contributes to failure of cold-induced beige adipocyte formation in old mice and humans. Cell Metab. 2017;25(1):166–81. https://doi.org/10.1016/j.cmet.2016.10.023.
16. Ritchie ME, Phipson B, Wu D, et al. limma powers differential expression analyses for RNA-sequencing and microarray studies. Nucleic Acids Res. 2015;43(7): e47. https://doi.org/10.1093/nar/gkv007.
17. Love MI, Huber W, Anders S. Moderated estimation of fold change and dispersion for RNA-seq data with DESeq2. Genome Biol. 2014;15(12):550. https://doi.org/10.1186/s13059-014-0550-8.
18. Garcia-Alonso L, Holland CH, Ibrahim MM, et al. Benchmark and integration of resources for the estimation of human transcription factor activities. Genome Res. 2019;29(8):1363–75. https://doi.org/10.1101/gr.240663.118.
19. Newman AM, Liu CL, Green MR, et al. Robust enumeration of cell subsets from tissue expression profiles. Nat Methods. 2015;12(5):453–7. https://doi.org/10.1038/nmeth.3337.

20. Hänzelmann S, Castelo R, Guinney J. GSVA: gene set variation analysis for microarray and RNA-Seq data. BMC Bioinformatics. 2013;14(1):7. https://doi.org/10.1186/1471-2105-14-7.
21. Zheng H, Song K, Fu Y, et al. An absolute human stemness index associated with oncogenic dedifferentiation. Brief Bioinform. 2021;22(2):2151–60. https://doi.org/10.1093/bib/bbz174.
22. Ao L, Zhang Z, Guan Q, et al. A qualitative signature for early diagnosis of hepatocellular carcinoma based on relative expression orderings. Liver Int. 2018;38(10):1812–9. https://doi.org/10.1111/liv.13864.
23. Kishida T, Ejima A, Yamamoto K, et al. Reprogrammed functional brown adipocytes ameliorate insulin resistance and dyslipidemia in diet-induced obesity and type 2 diabetes. Stem Cell Reports. 2015;5(4):569–81. https://doi.org/10.1016/j.stemcr.2015.08.007.
24. Moisan A, Lee Y-K, Zhang JD, et al. White-to-brown metabolic conversion of human adipocytes by JAK inhibition. Nat Cell Biol. 2014;17(1):57–67. https://doi.org/10.1038/ncb3075.
25. Barquissau V, Beuzelin D, Pisani DF, et al. White-to-brite conversion in human adipocytes promotes metabolic reprogramming towards fatty acid anabolic and catabolic pathways. Mol Metab. 2016;5(5):352–65. https://doi.org/10.1016/j.molmet.2016.03.002.
26. Singh AM, Zhang L, Avery J, et al. Human beige adipocytes for drug discovery and cell therapy in metabolic diseases. Nat Commun. 2020;11(1):2758. https://doi.org/10.1038/s41467-020-16340-3.
27. Mueez UD, Saari T, Raiko J, et al. Postprandial oxidative metabolism of human brown fat indicates thermogenesis. Cell Metab. 2018;28(2):207-16.e3. https://doi.org/10.1016/j.cmet.2018.05.020.
28. Lee MJ, Jash S, Jones JEC, et al. Rosiglitazone remodels the lipid droplet and britens human visceral and subcutaneous adipocytes ex vivo. J Lipid Res. 2019;60(4):856–68. https://doi.org/10.1194/jlr.M091173.
29. Liu X, Cervantes C, Liu F. Common and distinct regulation of human and mouse brown and beige adipose tissues: a promising therapeutic target for obesity. Protein Cell. 2017;8(6):446–54. https://doi.org/10.1007/s13238-017-0378-6.
30. Cypess AM, White AP, Vernochet C, et al. Anatomical localization, gene expression profiling and functional characterization of adult human neck brown fat. Nat Med. 2013;19(5):635–9. https://doi.org/10.1038/nm.3112.
31. Guenantin AC, Briand N, Capel E, et al. Functional human beige adipocytes from induced pluripotent stem cells. Diabetes. 2017;66(6):1470–8. https://doi.org/10.2337/db16-1107.
32. Rosenwald M, Perdikari A, Rulicke T, et al. Bi-directional interconversion of brite and white adipocytes. Nat Cell Biol. 2013;15(6):659–67. https://doi.org/10.1038/ncb2740.
33. Xiang AS, Meikle PJ, Carey AL, et al. Brown adipose tissue and lipid metabolism: new strategies for identification of activators and biomarkers with clinical potential. Pharmacol Ther. 2018;192:141–9. https://doi.org/10.1016/j.pharmthera.2018.07.002.
34. Wu J, Bostrom P, Sparks LM, et al. Beige adipocytes are a distinct type of thermogenic fat cell in mouse and human. Cell. 2012;150(2):366–76. https://doi.org/10.1016/j.cell.2012.05.016.
35. Zhou Z, Torres M, Sha H, et al. Endoplasmic reticulum–associated degradation regulates mitochondrial dynamics in brown adipocytes. Science. 2020;368(6486):54–60. https://doi.org/10.1126/science.aay2494.
36. Zhang G, Han J, Wang L, et al. The vesicular transporter STX11 governs ATGL-mediated hepatic lipolysis and lipophagy. iScience. 2022;25(4):104085. https://doi.org/10.1016/j.isci.2022.104085.
37. Oguri Y, Shinoda K, Kim H, et al. CD81 controls beige fat progenitor cell growth and energy balance via FAK signaling. Cell. 2020;182(3):563-77.e20. https://doi.org/10.1016/j.cell.2020.06.021.
38. Chondronikola M, Volpi E, Borsheim E, et al. Brown adipose tissue improves whole-body glucose homeostasis and insulin sensitivity in humans. Diabetes. 2014;63(12):4089–99. https://doi.org/10.2337/db14-0746.
39. Finlin BS, Memetimin H, Zhu B, et al. The beta3-adrenergic receptor agonist mirabegron improves glucose homeostasis in obese humans. J Clin Invest. 2020;130(5):2319–31. https://doi.org/10.1172/JCI134892.
40. Hanssen MJ, Hoeks J, Brans B, et al. Short-term cold acclimation improves insulin sensitivity in patients with type 2 diabetes mellitus. Nat Med. 2015;21(8):863–5. https://doi.org/10.1038/nm.3891.
41. Chouchani ET, Kazak L, Spiegelman BM. New advances in adaptive thermogenesis: UCP1 and beyond. Cell Metab. 2019;29(1):27–37. https://doi.org/10.1016/j.cmet.2018.11.002.
42. DeFronzo RA, Ferrannini E, Groop L, et al. Type 2 diabetes mellitus. Nat Rev Dis Primers. 2015;1:15019. https://doi.org/10.1038/nrdp.2015.19.

Publisher's Note